Analysis of Trace and Rare Earth Elements in Zircon at the Arizona LaserChron Center (G. Gehrels, 22 April 2023)

Analytical Methods

Trace and Rare Earth Elements in zircon provide a powerful tool for studying petrogenetic processes of igneous samples and for reconstructing provenance and source terrane characteristics for detrital samples. This document outlines the methods developed for analysis of trace and rare earth elements by LA-ICPMS at the Arizona LaserChron Center (ALC). Some aspects of the methodology have been reported by Chapman et al. (2016). Analyses are conducted with a Photon Machines G2 laser or a Teledyne Iridia laser connected to an Element2 ICPMS equipped with a Jet pump and interface (Pullen et al., 2018).

Our analytical method involves measurement of 23 trace and rare earth elements at the same time that eight U-Th-Pb (and Hg) isotopes are measured for U-Th-Pb geochronology. The isotopes measured include ^{27}Al, ^{29}Si, ^{31}P, ^{45}Sc, ^{49}Ti, ^{89}Y, ^{93}Nb, ^{139}La, ^{140}Ce, ^{141}Pr, ^{146}Nd, ^{152}Sm, ^{153}Eu, ^{157}Gd, ^{159}Tb, ^{164}Dy, ^{165}Ho, ^{166}Er, ^{169}Tm, ^{174}Yb, ^{175}Lu, ^{177}Hf, ^{181}Ta, ^{202}Hg, ^{204}(Hg+Pb), ^{206}Pb, ^{207}Pb, ^{208}Pb, ^{232}Th, and ^{235}U. Dwell times of these elements range from 0.001 sec to 0.300 sec, depending on expected concentrations, such that concentration measurements for a typical zircon should have a precision of better than 5% and U-Th-Pb ages should be reliable to ~2%. Analyses are conducted with six jumps in magnet setting during each scan. Dwell and settle times (shown as settle/dwell time in seconds) are as follows:

Al27=0.30/0.004	Nd146=0.001/0.004	Lu175=0.001/0.002
Si29=0.001/0.002	Sm152=0.001/0.004	Hf177=0.001/0.002
P31=0.001/0.002	Eu153=0.001/0.100	Ta181 = 0.001/0.002
Sc45=0.026/0.002	Gd157=0.001/0.002	Hg202=0.018/0.010
Ti49=.001/0.100	Tb159=0.001/0.002	(Hg+Pb)204=0.001/0.010
Y89=0.042/0.002	Dy164=0.001/0.002	Pb206=0.001/0.02
Nb93=0.001/0.01	Ho165=0.001/0.002	Pb207=0.001/0.02
La139=0.034/0.300	Er166=0.015/0.002	Pb208=0.001/0.002
Ce140=0.001/0.010	Tm169=0.001/0.002	Th232=0.001/0.002
Pr141=0.001/0.004	Yb174=0.001/0.002	U235=0.001/0.005

Each acquisition consists of 56 scans, each of which takes 1.1 seconds, for a total analysis time of ~60 seconds. This includes ~14 scans with the laser off to measure backgrounds, 37 scans with the laser firing to measure peak intensities, followed by 5 scans for sample washout. Analyses are conducted with a 35 micron laser beam diameter, a rep rate of 8 hz, and a fluence of ~7 J/cm^2, which yields laser pits that are ~30 microns deep.

Data reduction is accomplished with TREEcalcML, which is modified from E2agecalc, our in-house data-reduction system that operates in Excel (Gehrels et al., 2008; Pullen et al., 2018), and a similar routine that runs in MATLAB (E2agecalcML). Rather than using the data from Thermo FIN2 files, we use a python-based decoding routine that extracts raw intensities from .dat files (Hartman et al., 2017). This allows calculation of an Analog Conversion Factor (ACF) for each isotope and for each scan, which significantly improves data quality. Intensities (and acquisition times) from decoded dat files are imported into TREEcalcML along with a scancsv file that contains information about each analysis (e.g., sample name, grain number, spot location, focus settings). U-Th-Pb (and Hg) results are processed utilizing E2agecalc or E2agecalcML.

Results from analysis of T/REE analyses are reported in a variety of Excel spreadsheets that present both raw and reduced data.

Internal Calibration Using Si

The first correction applied to the data is a Si-based normalization. This is accomplished by calculating the average intensity (cps) of ^{29}Si in all analyses of our standard Sri Lanka zircon during a session, and then calculating an internal normalization factor that sets the ^{29}Si intensity of each unknown to the same value (Eqn #3 of Lin et al., 2016). The corrected intensity of ^{29}Si for each unknown is then divided by the stoichiometric concentration of ^{29}Si in zircon (7,179 ppm; Wiedenbeck et al., 2004) or NIST 612 (15,762 ppm; Jochum et al., 2012), resulting in a factor that relates signal intensity (cps) to concentration (ppm). This factor is then applied to all other isotopes in the same analysis, resulting in Si-normalized concentrations. This is referred to as an internal correction because it relies only on the intensities measured during an individual analysis, and the assumption that Si in zircon is approximately stoichiometric. It accounts for spot-to-spot variations in sensitivity due to variations in the laser (laser energy & focus), the mass spec (e.g., sensitivity drift, which is due largely to variations in gas flows, temperatures, tune settings), and the sample (e.g., ablation across fractures, inclusions, or epoxy). It does not correct for accidental analysis of inclusions.

External Calibration Using FC-1, Sri Lanka, R33 Zircon and NIST612 Glass

The second correction is based on analysis of FC-1, Sri Lanka, and R33 zircon standards and NIST612 (trace element glass) during the analytical session. This is an external calibration, much like primary standard-sample bracketing for calibrating U-Th-Pb geochronologic data by LA-ICPMS. Concentrations of T/REE in FC-1, Sri Lanka, R33 have been determined in-house by comparison with concentrations of 91500 and MAD559 zircons, which have been reported by Coble et al. (2018). Calibration utilizing these materials is not ideal given that: (1) concentrations of T/REE in 91500 and MAD559 were determined by both LA-ICPMS and SIMS, and the results differ in many cases, (2) concentrations for some elements have large uncertainties, (3) the concentrations of some elements (e.g., La and Pr) in 91500 are extremely low, approaching detection limit for our system, and (4) we need to use secondary reference materials (FC-1, SL, and R33) because quantities of 91500 and MAD559 are limited. SL is used as our primary standard because it is more homogeneous that Fc-1 and R33, and has higher concentrations of La and Pr.

NIST612 is a trace element glass that has ~30 ppm of all elements of interest. This raises the possibility of calibrating with NIST612, but information from NIST612 is not directly comparable to analysis of zircons because NIST612 has a glass matrix, which results in total sensitivity, sensitivity drift, and elemental/isotopic fractionation that are different from zircon.

TREEcalcML provides the option of performing the external calibration with either SL or FC-1, or some combination of the two. It also shows the impact on determined R33 and NIST612 concentrations. This is shown on the Calibration Plot and the Offset Plot on the TREECalcML interface.

TREEcalcML Output

TREEcalcML outputs a variety of figures and tables that can be used to evaluate data quality, and for interpretation of data. These are saved in the original folder that contains the scancsv and xls files. The various tables include:

-- AnalysisValue Table: shows all intensities for each analysis. Labels indicate which rows are used for background intensities, PeakValue intensities, Tzero, stability determination, and the rows used to determine concentrations.

-- PeakValue Table: shows all intensities use to determine peak intensities for each analysis. Labels indicate which rows are used for Tzero, stability determination, and the rows used to determine concentrations. Below the data table are values from Si normalization and standard calibration.

-- TREEppm Data Table: Concentrations of all elements in ppm

-- TREEnorm Data Table: Chondrite-normalized concentrations of all elements in ppm

-- TREE WR Data Tables: Show whole-rock concentrations utilizing a variety of partition coefficients.

TREEcalc also exports all of the figures from the graphical user interface as pdf files.

T/REE Data Interpretation

There are many different ways to use T/REE concentrations from zircon. Following are just a few examples.

Petrogenesis of Igneous Rocks

Excellent summaries of utilizing T/REE geochemistry to determine igneous petrogenesis have been published by Bell et al. (2016), Belousova et al. (2002), Grimes et al. (2015), Trail et al. (2016), and many others. Following are some examples utilizing data from the Coast Mountains Batholith.

Figure 1. Chondrite-normalized concentrations of REE from various plutons. Also shown are measured (solid lines) and known concentrations (dotted lines) of 91500 and NIST612.

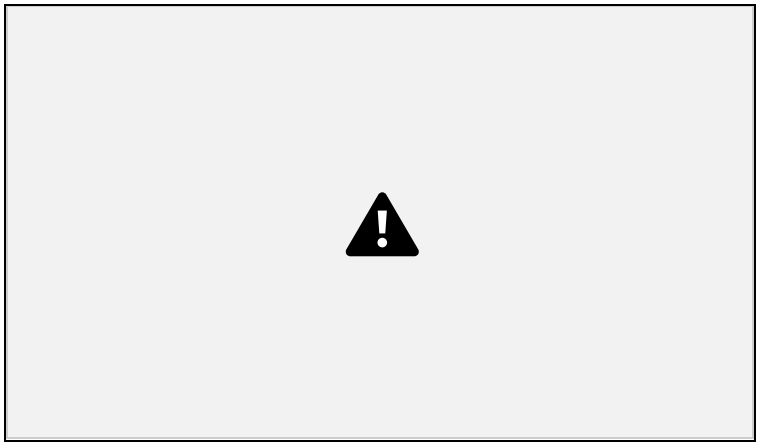

Figure 2. Crystallization temperature and crustal thickness determined from Ti concentrations and La/Yb concentrations (respectively) measured in zircon. Crystallization temperature is calculated following Watson and Harrison (2006); crustal thickness is calculated following Profeta et al. (2015).

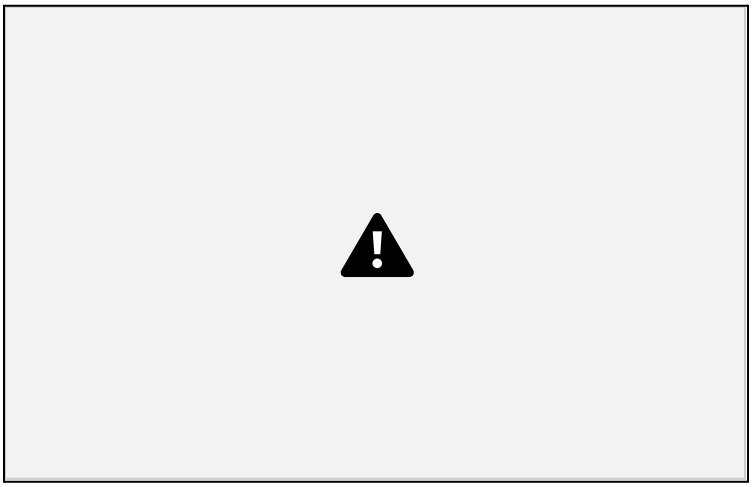

Figure 3. Diagram showing the distinct Ce and Eu concentrations of igneous rocks of variable composition (following Belousova et al. 2002).

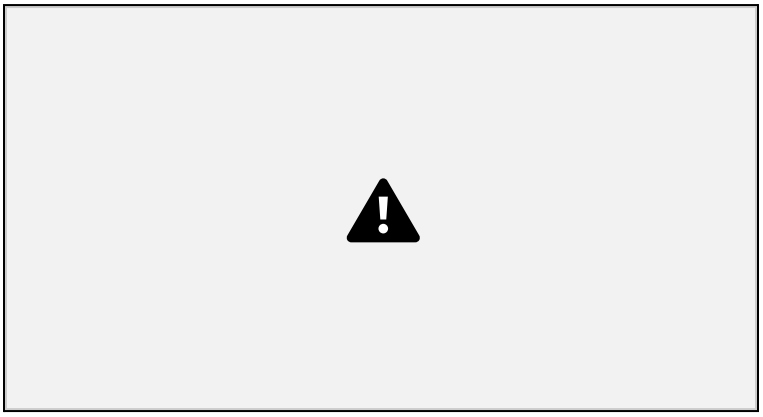

Figure 4. Compositional fields of igneous rocks on a Nb-Ta discrimination diagram (following Belousova et al., 2002).

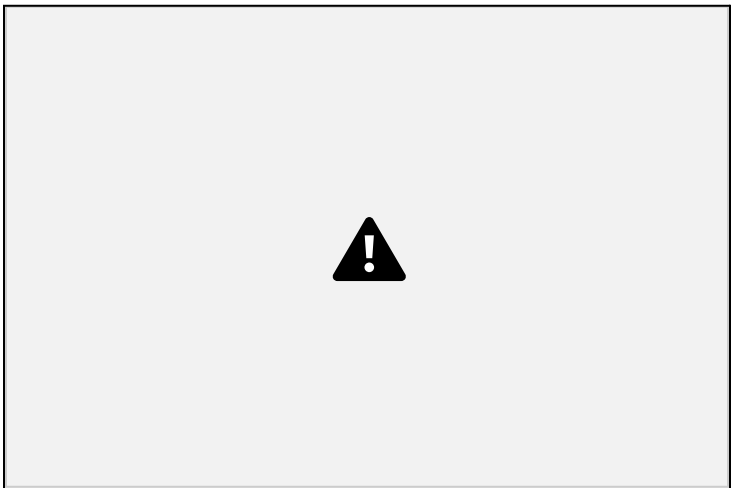

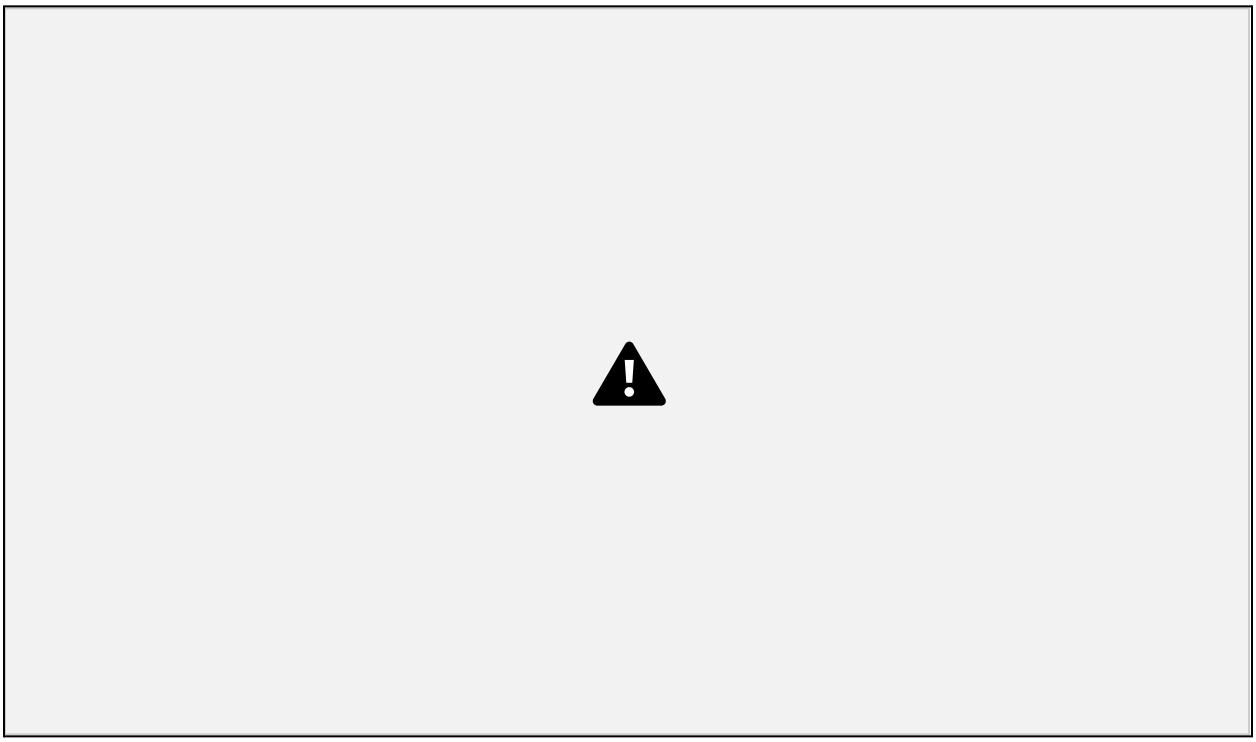

Figure 5. Being able to use whole-rock concentrations of REE opens up additional methods of analysis. This plot shows the variation in whole-rock concentrations of eleven different plutonic rock samples from the Coast Mountains Batholith using the partition coefficients of Chapman et al. (2016).

Analysis of Detrital Zircons

Following are some examples of the use of T/REE data from a Cretaceous sandstone from the Colorado Plateau (CP39) that contains grains derived from many different provinces of North America. As described by Dickinson et al. (2008), grains are interpreted to have been shed from Archean, 2.0-1.72 Ga, 1.72-1.60 Ga, ~1.4 Ga, and 1.4-1.2 Ga basement provinces of North America; the Grenville (1.2-1.0 Ga) orogen, Appalachian (500-400 Ma) orogen, and peri-Gondwana terranes (800-500 Ma) of eastern Laurentia; the Ouachita orogen (400-300 Ma

grains), the east Mexico arc (300-250 Ma); and Jurassic and Cretaceous arc systems along the Cordilleran margin. Figures 6-9 show some of the T/REE characteristics that could be used to characterize these source regions for provenance studies, or, if provenance is known, to study petrogenesis of the igneous host rocks. 315 grains were analyzed.

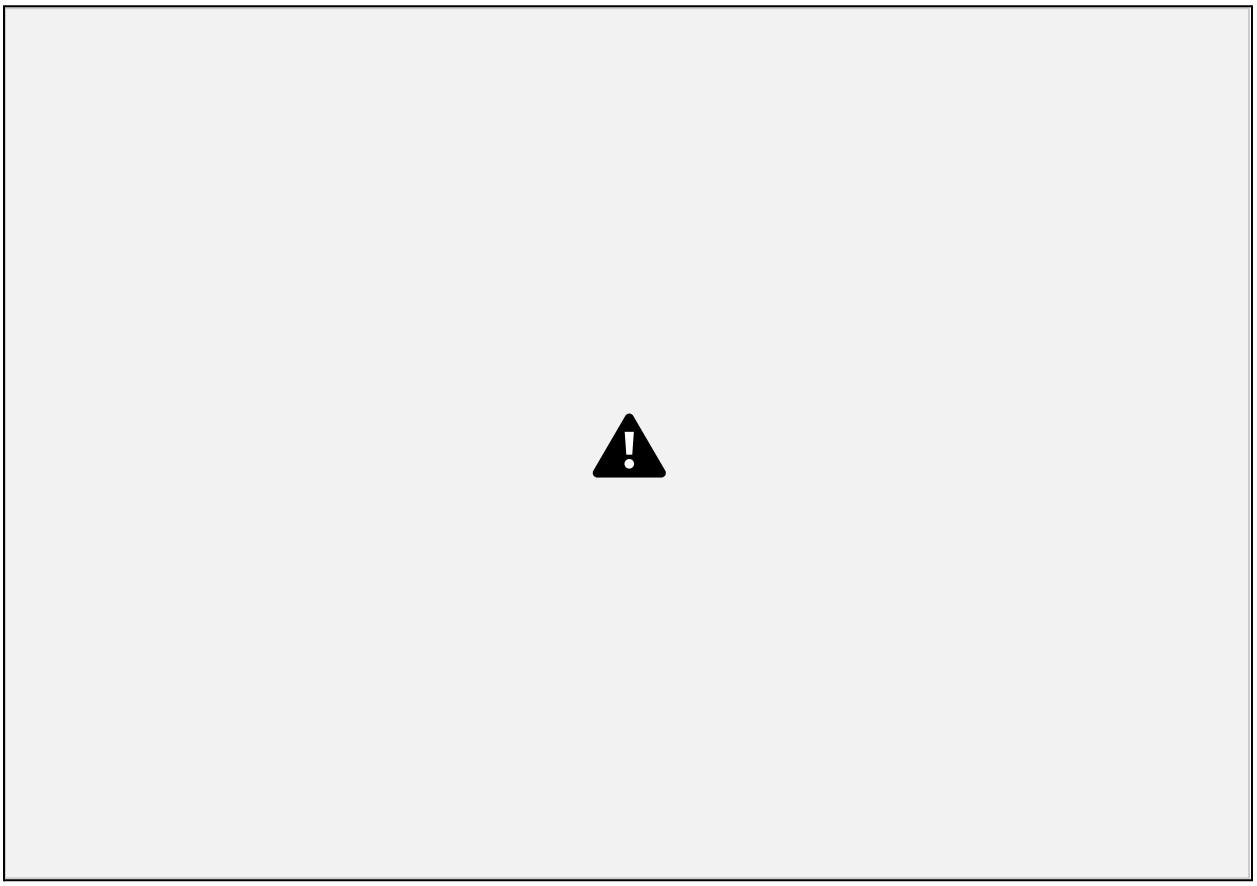

Figure 6. Chondrite-normalized T/REE concentrations from a detrital zircon sample. Shown are average concentrations for each age group.

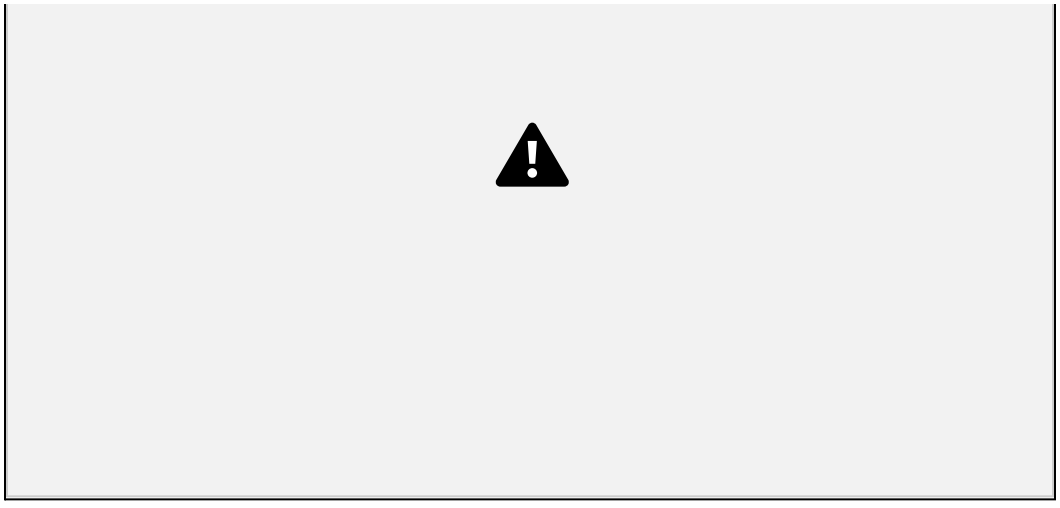

Figure 7. Plot showing calculated crustal thickness based on La/Yb (Profeta et al., 2015) and crystallization temperature based on Ti concentrations (Watson and Harrison, 2006). Symbols are averages of all values for each group, ellipses encircle most individual analyses. Calculated thickness values are a good match with tectonic history (e.g., thicker crust in Appalachian and 1.8-2.0 Ga orogens, thinner crust in the Jurassic arc).

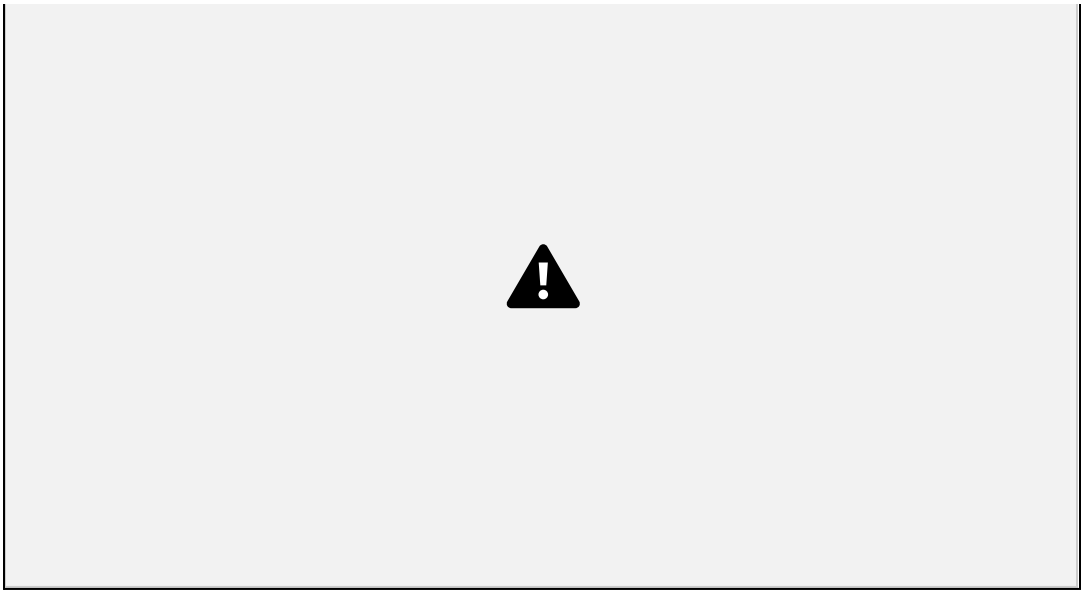

Figure 8. Nb-Ta discrimination diagram (from Belousova et al. (2002). Ellipses include most analyses of each group, symbols are average values.

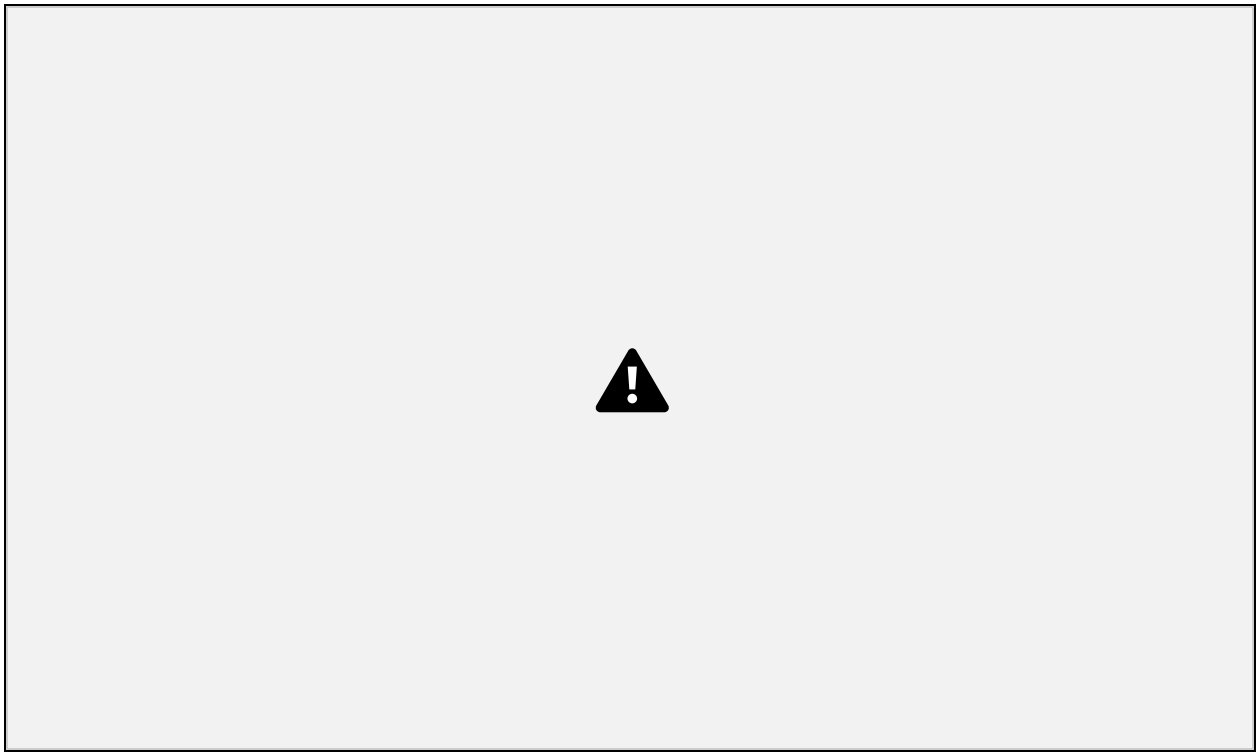

Figure 9. Plot of La versus Sm/La, which is useful for determining whether a zircon has been affected by hydrothermal alteration. Such analyses should be excluded from determination of magmatic concentrations. Diagram from Hoskin (2005), Fu et al. (2009), and Bell et al. (2016).

cogenetic, which would statistical analysis of the youngest grains that are truly coeval (e.g., Gehrels et al., 2006; Gehrels, 2012).

References Cited

Bell, E.A., Boehnke, P., and Harrison, T.M., 2016, Recovering the primary geochemistry of Jack Hills zircons through quantitative estimates of chemical alteration: Geochimica et Cosmochimica Acta, v. 19, p. 187-202.

Belousova, E.A., Griffin, W.L., O'Reilly, S.Y., Fisher, N.J., 2002, Igneous zircon: trace element composition as an indicator of source rock type: Contributions to Mineralogy and Petrology, v. 143, p. 602–622.

Chapman, J., Gehrels, G., Ducea, M., Giesler, D., Pullen, A., 2016, A new method for estimating parent rock trace element concentrations from zircon: Chemical Geology, v. 439, p. 59-70.

Coble, M., Vazquez, J., Barth, A., Wooden, J., Burns, D., Kylander-Clark, A., Jackson, S., and Vennari, C., 2018, Trace element characterization of MAD-559 zircon reference material for ion microprobe analysis: Geostandards and Geoanalytical Research.

Dickinson, W.R., Gehrels, G.E., 2008, Sediment delivery to the Cordilleran foreland basin: Insights from U-Pb ages of detrital zircons in Upper Jurassic and Cretaceous strata of the Colorado Plateau: American Journal of Science, v. 308, p. 1041-1082.

Fu, B., Mernagh, T., Kita, N., Kemp, A., Valley, J., 2009, Distinguishing magmatic zircon from hydrothermal zircon: A case study from the Gidginbung high-sulphidation Au–Ag–(Cu) deposit, SE Australia: Chemical Geology, v. 259, p. 131-142.

Gehrels, G., 2012, Detrital Zircon U-Pb Geochronology: Current Methods and New Opportunities, in Tectonics of Sedimentary Basins: Recent Advances, C. Busby and A. Azor, editors, Wiley-Blackwell Publishing, p. 47-62.

Gehrels, G.E., Valencia, V., Pullen, A., 2006, Detrital zircon geochronology by Laser-Ablation Multicollector ICPMS at the Arizona LaserChron Center, in Loszewski, T., and Huff, W., eds., Geochronology: Emerging Opportunities, Paleontology Society Short Course: Paleontology Society Papers, v. 11, 10 p.

Grimes, C.B., Wooden, J.L., Cheadle, M.J., and John, B.E., 2015, "Fingerprinting" tectono-magmatic provenance using trace elements in zircon: Contributions to Mineralogy and Petrology, v. 170, p. 1-26.

Hartman, J., Franks, R., Gehrels, G., Hourigan, J., and Wenig, P., 2017, Decoding dat files from a Thermo Element™ ICP Mass Spectrometer: Archive.org.

Jochum, K., Weis, U., Stoll, B., Kuzmin, D., Yang, Q., Raczek, I., Jacob, D., Stracke, A., Birbaum, K., Frick, D., Gunther, D., and Enzweiler, J., 2011, Determination of reference values for NIST 610-617 glasses following ISO guidelines: Geostandards and Geoanalytical Research, v. 35 (4), p. 397-429.

Profeta, L., Ducea, M.N., Chapman, J.B., Paterson, S.R., Henriquez, S.M., Kirsch, M., Petrescu, L., DeCelles, P.G., 2015. Quantifying crustal thickness over time in magmatic arcs. Sci. Report. 5.

Pullen, A., Ibanez-Mejia, M., Gehrels, G., Giesler, D., and Pecha, M., 2018, Optimization of a laser ablation–single collector–inductively coupled plasma–mass spectrometer (Thermo Element 2) for accurate, precise, and efficient zircon U-Th-Pb geochronology: Geochemistry, Geophysics, Geosystems. V. 19.

Trail, D., Tailby, N., Wang, Y., Harrison, T.M., and Boehnke, P., 2016, Aluminum in zircon as evidence for peraluminous and metaluminous melts from the Hadean to present: Geochemistry, Geophysics, Geosystems, v. 18, doi:10.1002/2016GC006794.

Watson, E.B., and Harrison, T.M., 2005, Zircon thermometer reveals minimum melting conditions on earliest Earth: Science, v. 308, p. 841-844.

Wiedenbeck, M., Hanchar, J.M., Peck, W.H., Sylvester, P., Valley, J., Whitehouse, M., Kronz, Morishita, Y., and Nasdala, L., 2004, Further characterization of the 91500 zircon crystal: Geostandards and Geoanalytical Research, v. 28, p. 9–39.